Supporting Information

The Role of the Electron Spin Polarization in Water Splitting

Wilbert Mtangi, Vankayala Kiran, Claudio Fontanesi, and Ron Naaman

Dept. of Chemical Physics, Weizmann Institute of Science

Rehovot 76100, Israel

Preparation of TiO_2 electrodes

TiO_2 nanoparticulate films were deposited on fluorine-doped tin oxide (FTO, surface resistivity of ~7 Ω/sq,) coated glass, purchased from Sigma Aldrich Co., using the electrophoretic deposition (EPD) technique. This technique has been used previously to deposit uniform TiO_2 films[1,2,3,4,5]. A suspension of TiO_2 nanoparticles (NPs) was prepared by dispersing 0.4g TiO_2 NP (<25nm in diameter and 99.7% trace metals, from Sigma Aldrich) in 40 mL of de-ionized water. Prior to making dispersions, TiO_2 nanoparticle powders were heated at 300°C for 1 hr. The mixture was stirred overnight to ensure homogeneity. Prior to nanoparticle deposition, the FTO substrates were boiled in isopropanol for 15 minutes, followed by 15 minutes of boiling in ethanol, and finally rinsed with de-ionized water. After having been rinsed, the substrates were dried using nitrogen gas and annealed for 15 minutes at T=570 K. EPD was then performed with a Princeton potentiostat using the galvanic pulses mode technique with two pulses (Pulse 1 and Pulse 2).

Pulse 1 was set to 0 mA for 200 s for depolarization. Pulse 2 has current values ranging from 0.50 to 0.95 mA (producing a maximum potential of 7.0 V). Pulse 2 was applied for 1000 s in each cycle for polarization, and the number of iterations (pulse 1 followed by pulse 2) was set to 750. Various cycles were used to prepare films of required thicknesses. The samples were annealed in between cycles at 570 K for 15 minutes in air. During EPD, the suspension was continuously stirred using a magnetic stirrer. After completion of the last cycle, the electrodes were annealed again for 8 hrs.

To confirm the surface coverage of the EPD-deposited TiO_2 NP on FTO, high-resolution scanning electron microscope (SEM) measurements were performed using In-lens-detector

imaging with a LEO-Supra 55 VP. The SEM images in Figure S1 show a high surface coverage of the TiO_2 NP on FTO substrates deposited using the EPD technique. An average film thickness of around 6.8 µm was measured, using the Dektak stylus profilometer.

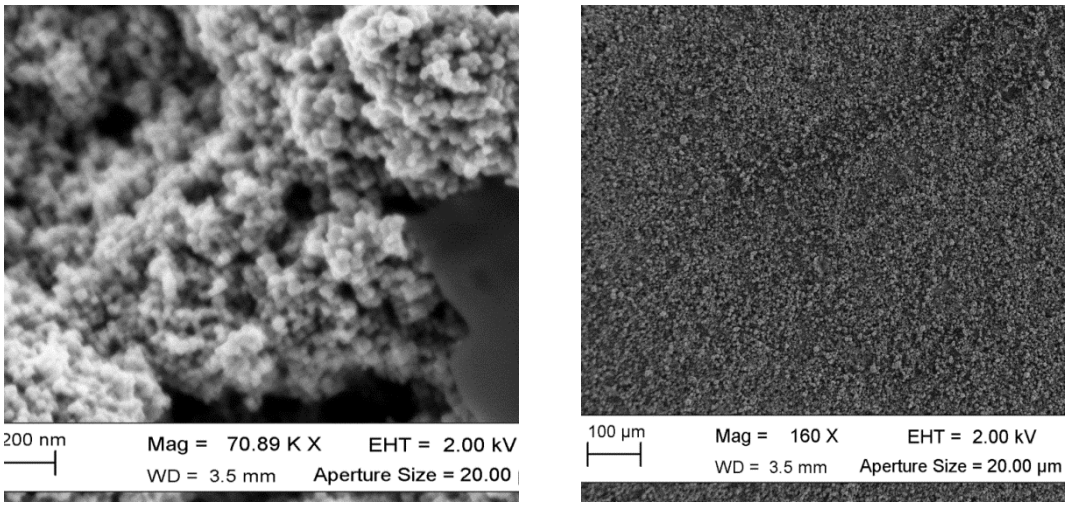

Figure S1: SEM images of EPD coated TiO_2 nanoparticles on FTO under two different magnifications.

Functionalization of the electrode by the linker molecules

TiO_2 films were functionalized using organic linker molecules in order to attach the CdSe NP. In this study, (COOH)-(Ala-Aib)$_5$-NH-(CH$_2$)$_2$-SH (Al5), (COOH)-(Ala-Aib)$_7$-NH-(CH$_2$)$_2$-SH (Al7), 11-mercapto-undecanoic acid (MUA), 3-mercaptobenzoic acid (3 MBA), 4-mercaptobenzoic acid (4 MBA), and 3-mercaptopropionic acid (MPA) were used as linkers. The oligopeptide was dissolved in dimethyl formamide (DMF) to afford a 0.10 mM solution, whereas MPA and MUA were dissolved in ethanol to afford 5 and 1 mM solutions, respectively. 3 MBA and 4 MBA were also dissolved in ethanol to afford 1 mM solutions. The 1.0 x 1.5 cm^2 electrodes coated with TiO_2 were then immersed into the linker molecule solutions for an incubation period of 48 hrs. The linker molecules are attached to the TiO_2 surface by their carboxylic group.[6,7,8]

Modification of electrodes with dsDNA

We used single-stranded DNA, a 40-base oligonucleotide (40 bp) with the following sequence: 5'-AAA GAG GAG TTG ACA GTT GAG CTA ATG CCG ATT CTT GAG A/3AmMO/ -3' and complementary DNA (comp-DNA) oligomer with the sequence 5'- TCT CAA GAA TCG GCA TTA GCT CAA CTG TCA ACT CCT CTT T/3ThioMC3-D/ -3'. 200µL of double-

stranded DNA was prepared by mixing 20µL of the HS-ssDNA with 22µL of its complementary DNA from a stock solution of 100µM. The mixture was kept in PCR, which was heated to a temperature of 372K and allowed to cool down to room temperature, overnight. Thereafter, 70 µL of the solution was adsorbed on the TiO_2 electrodes.

Prior to adsorption of the dsDNA molecules, the electrodes were cleaned using ethanol and water. The surface was functionalized using terephtalic acid. To this end, 10 mM of terephtalic acid solution was prepared in 10 mL of water and 100 µL of triethylamine. The electrodes were incubated in the terephtalic acid solution for 12 hours, followed by rinsing with water. The previously functionalized surface for amide bond formation with the dsDNA was then activated by incubating the electrodes in a mixture of 60 mM N-Hydrosuccinimide and 30 mM ethyl-N,N-dimethylcarbodiimide, which was dissolved in 0.8 M phosphate buffer. Electrodes were incubated for 15 hrs.

Finally, the dsDNA was adsorbed by keeping the electrodes for 24 hrs in a controlled humidified environment, after which the samples were rinsed with 0.4 M phosphate buffer and de-ionized water to remove any excess of DNA and salts. They were then blown dry using nitrogen gas. The electrodes were then immersed into the CdSe nanoparticle solution for at least 3 hrs.

Adsorption of CdSe nanoparticles

CdSe NP (~ 7 nm diameter from MK Impex Corp.) was used in this study. The MKN-CdSe-T640 nanoparticle dispersion was mixed with toluene to afford a concentration of 22.5 mM. The functionalized TiO_2 electrodes were then incubated in the CdSe nanoparticle dispersions for at least 3 hrs to ensure the adsorption of CdSe NP to the S-terminal of the linker molecules. The electrodes were then rinsed thoroughly in toluene to remove the physisorbed NP, and finally dried with nitrogen gas.

Transmission Electron Microscopy

Samples for TEM analysis were prepared by drop casting 5 μL toluene dispersions of TiO_2-oligopeptide-CdSe onto a carbon-coated copper grid, followed by air drying. Prior to TEM measurements, the samples were kept in vacuum for 12 hrs. TEM was performed on a Philips T12 transmission electron microscope operating at 120 kV and equipped with a TVIPS CCD digital camera.

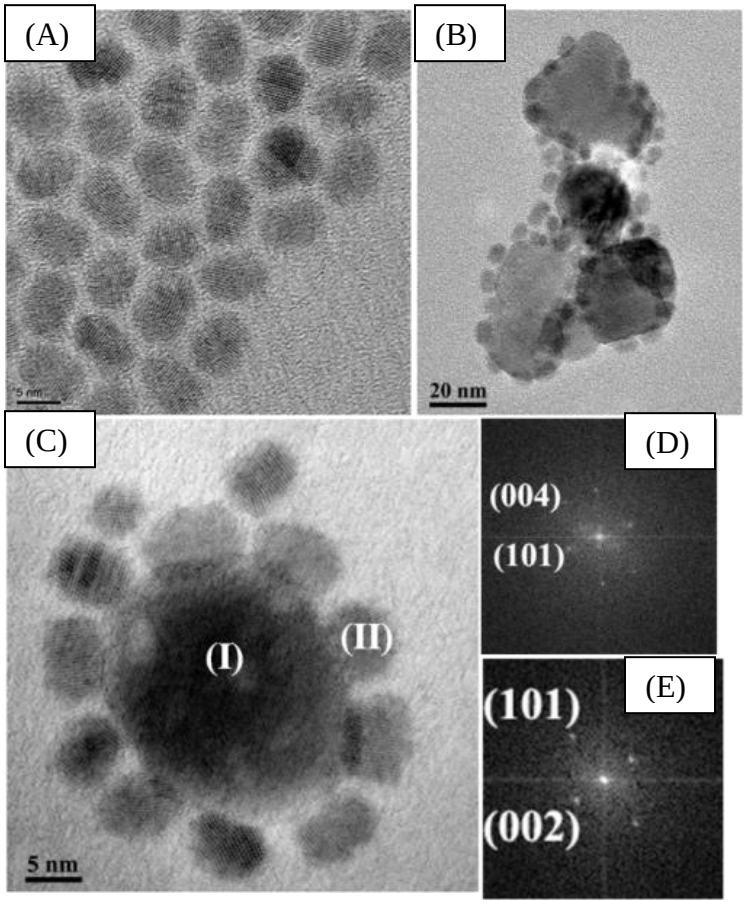

Figure S2: TEM images of (A) CdSe nanoparticles (scale bar is 5 nm). (B,C) CdSe anchored to TiO_2 nanoparticles. As clearly shown, several CdSe nanoparticles are attached to one TiO_2 particle. (D) The FFT pattern obtained from regions marked as I (image C) and (F) the FFT pattern obtained from region II (image D). The FFT images confirm the crystalline structure of the particles used.

The films were characterized using UV-Vis absorption measurements to confirm the presence of CdSe NP. As shown in Figure S3, the spectra reveal the presence of a peak around 635 nm, corresponding to CdSe NP. This peak is almost unaltered even after the NPs are anchored onto the TiO_2 NP, confirming the formation of the TiO_2/linker/CdSe structure. In addition, it is noteworthy that the peak intensities are very similar (within 10%), indicating that the CdSe NP coverage in all samples is similar.

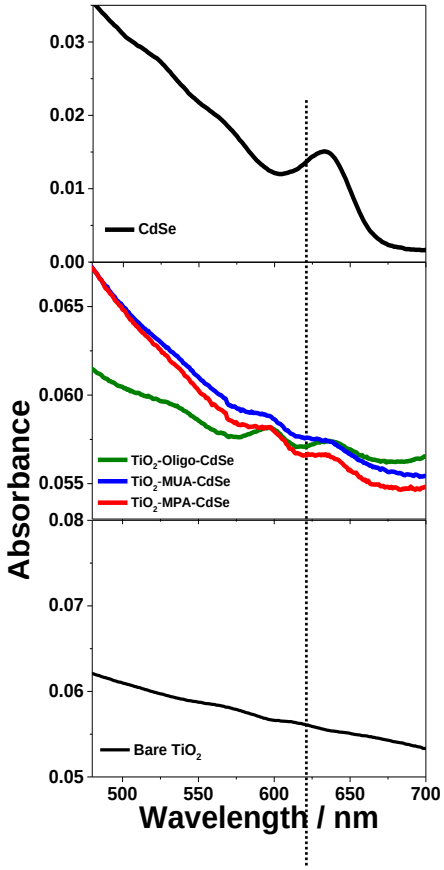

Figure S3: Absorption spectra of CdSe NP dispersed in toluene (top); of a structure of CdSe/linker/TiO_2 films (middle) and of a bare TiO_2 film (bottom).

Room temperature photoluminescence measurements were performed using a green laser (514.5 nm). The PL measurements were performed using a LabRam HR800-PL microscope (Horiba Jobin-Yvon). They were carried out with a slightly opened confocal hole (400µm) and an integration time of 2 seconds.

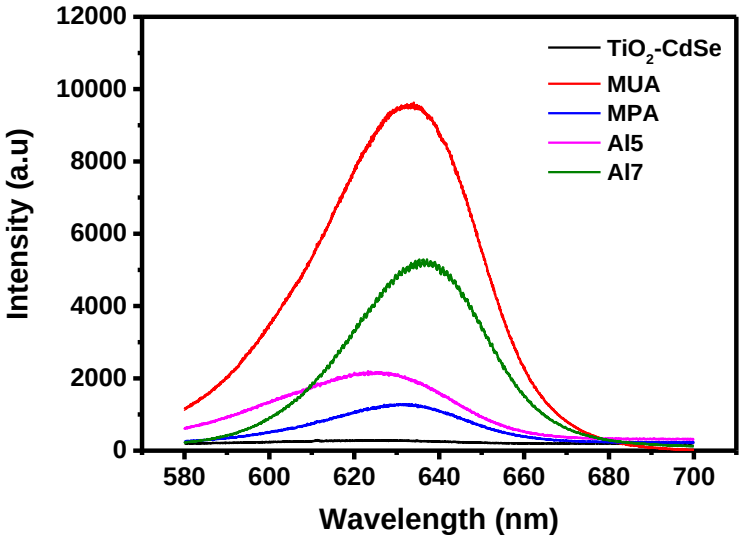

Figure S4: Photoluminescence as a function of wavelengths obtained from CdSe nanoparticles adsorbed on TiO_2 using the three different linkers. Measurements were performed at room temperature using a 514.5 nm laser.

Spin selectivity in electron transmission through the oligopeptide

To confirm the spin selectivity of the electron transmission through the oligopeptides used in this study, conductive probe AFM (CP-AFM) measurements on molecules adsorbed on a Ni substrate were performed.

Nickel substrate preparation

Thin films of nickel (Ni) metal were prepared using the e-beam evaporation technique. Briefly, 200 nm Ni (Kurt, 99.9%) was evaporated onto pre-deposited Ti (8-nm), which acts as an adhesion layer. The Ti/Ni coatings were deposited sequentially on silicon wafers without breaking the base vacuum in the electron-beam evaporator, at a base pressure of about 1 x 10^{-6} mbar. The evaporation was controlled at a rate of 0.2 Å/s for Ti and 2.0 Å/s for Ni.

Oligopetide monolayers on Ni

Self-assembled monolayers of oligopeptides were adsorbed on nickel substrates. Prior to the immobilization of the self-assembled monolayer, thin Ni films were thoroughly cleaned by

placing them in boiling acetone and ethanol for 20 minutes each. Finally, the cleaned Ni samples were dipped in 0.1 mM solution of oligopeptide in dimethyl formamide for 24 hours.

The presence of oligopeptides on the Ni surface was confirmed using polarization-modulated infrared absorption spectroscopy (PMIRRAS) and atomic force microscopy. Infrared absorption spectroscopy in reflection mode was carried out using a Nicolet 6700 FTIR, at an incidence angle of 80^{o}, equipped with a PEM-90 photo elastic modulator (Hinds Instruments, Hillsboro, OR). Raw spectra were baseline-corrected by a spline algorithm. As shown in Figure S4, the PMIRRAS data represent two peaks located at 1660 and 1550 cm^{-1}. The former is due to C=O stretching vibration, commonly termed amide I, and the latter is derived from the C-N stretching mode and the bending mode of N-H bond (amide II) present in oligopeptide. The presence of these peaks confirms the formation of an oligopetide monolayer on the Ni surface. In addition, the positions and the relative intensity ratio dictate the conformation of the peptide monolayer adsorbed on the Ni surface.

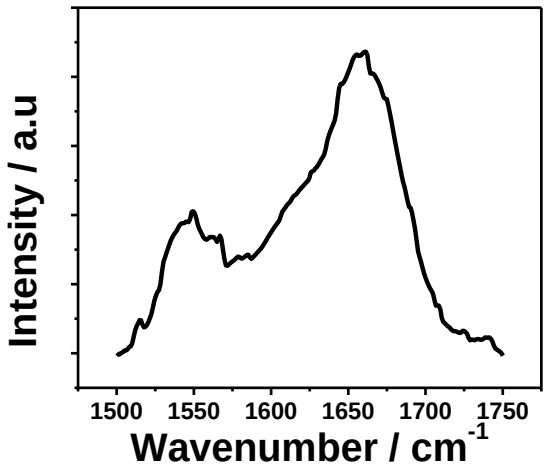

Figure S5: PMIRRAS spectrum of an oligopeptide monolayer on a nickel surface

AFM measurements

Microscopic transport measurements were performed using CP-AFM under different magnetic orientations. The measurements were carried out using a Multimode/Nanoscope (Bruker-Nano, Santa Barbara, CA USA). A PtIr-coated Si probe (Bruker, SCM-PIT, spring constant 1-5 N/m) was used. Peak force TUNA (PF-TUNA)^{TM} mode was used for acquiring current (I) versus voltage curves (V) curves. In PF-TUNA mode, the tip taps on the surface at a frequency of 1

kHz, controlling the peak contact force (here, held to a few nN) at each tap; thus the tip forms a molecular junction. The tip simultaneously scans the surface at a rate of 1 Hz per scan line. I-V spectroscopy measurements were recorded by performing voltage ramps with the tip in contact with the surface at an applied force of about 5 nN. Using the ramping software, the tip was lifted between spectroscopy points at different places on the surface. At least 25 I-V curves were averaged for each configuration (Magnet UP and Magnet DOWN) by leaving spectra that exhibit shorting and insulating behavior.

Prior to I-V measurements, the nanoshaving method is utilized to measure the thickness of the oligopeptide monolayer on the Ni surface. A defined area (1 μm x 1 μm) is scanned in contact mode by applying a large force on the AFM tip, which removes molecules present in that area due to their inherent flexibility of molecules, as shown in Figure S6. From the line profile, the thickness of the monolayer was found to be 2.8±0.2 nm.

The spin selectivity in electron transmission through the oligopeptide was verified by CP-AFM measurements as reported earlier.[9,10,11] The permanent magnet was applied so that the nickel was magnetized with its magnetic field pointing either up or down. The current-versus-voltage curves were recorded when the AFM tip was in contact with the monolayer of the oligopeptide. Figure S7 presents the current (I) versus the voltage (V) curves, when the potential is applied between the AFM tip and the Ni substrate. The results reveal clear spin selectivity in electron transmission. The ratio varies from sample to sample and the error reflects this variation.

The asymmetry in the spin filtering is attributed to the change in the molecular structure upon applying the voltage. This change depends on the alignment of the molecule dipole relative to the applied field.[12] These measurements confirm the spin selectivity of electron transfer through the oligopeptides used in the present study. The spin polarization measured is 18±5%, 25±5% and 80±5%[10] for Al5, Al7, and DNA samples, respectively. The polarization is defined as the difference in the current of the two spins over their sum.

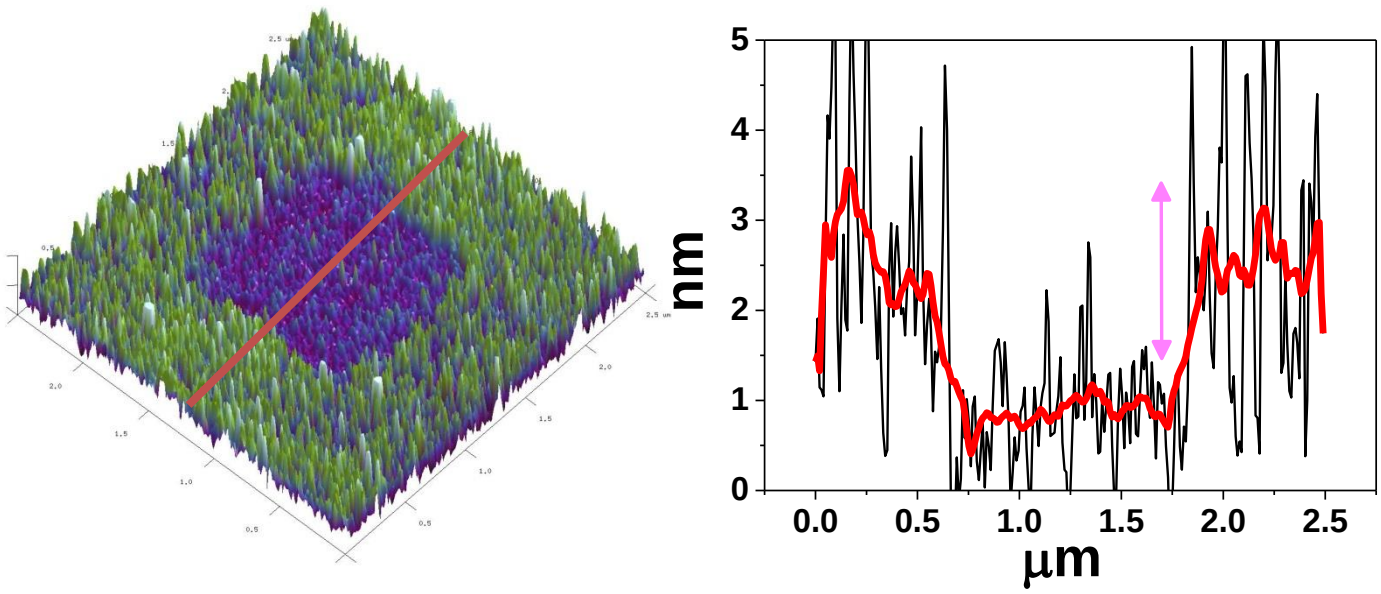

Figure S6: On the left- AFM topography of a monolayer of oligopeptide adsorbed on nickel The monolayer was removed from an area of 1 µm x 1 µm by the nanoshaving method, enabling us to estimate the thickness of the monolayer. The height profile was taken along the red line and is shown in the right figure. The thickness of the monolayer was 2.8±0.2 nm.

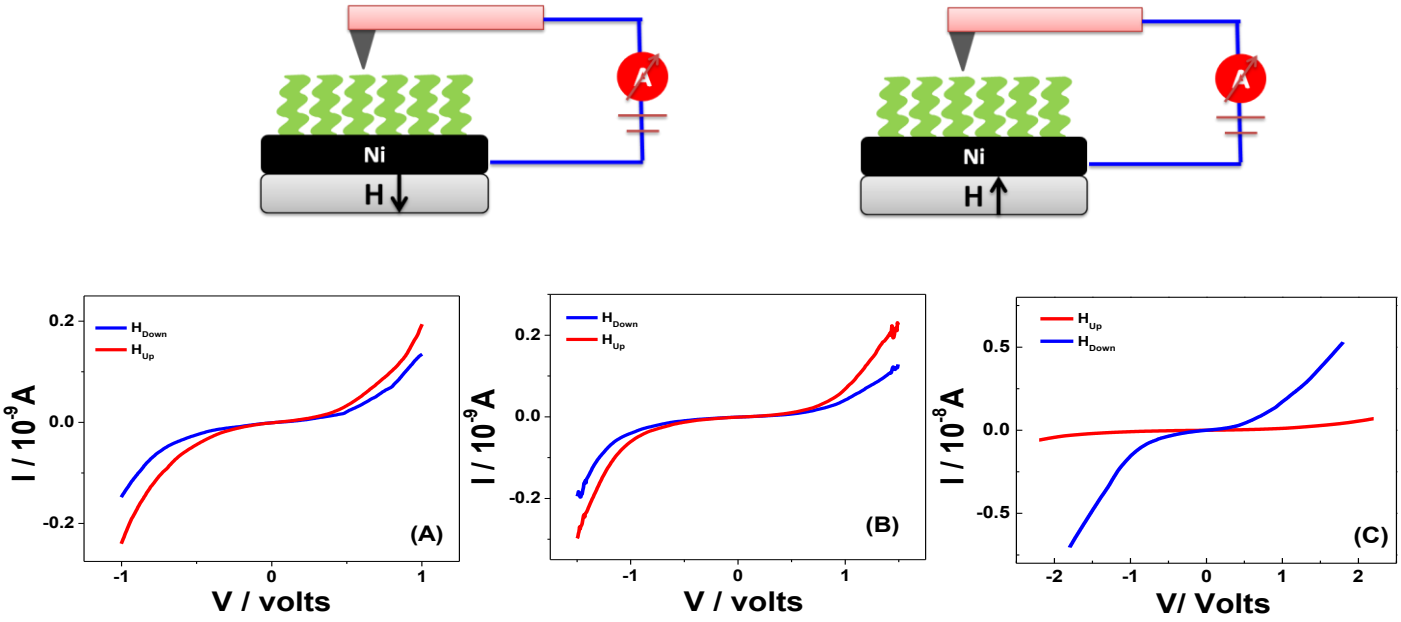

Figure S7. Top: Schemes of the experimental set-up for the two orientations of the magnetic field. Current (I) vs. voltage (V) curves obtained for (A) Al5, (B) Al7 and (C) 40 bp DNA[10] monolayers adsorbed on Ni by placing the magnet down and up. Blue- magnet DOWN and Red- magnet UP. The data represents an average of around 50-70 I-V curves obtained for oligopeptide monolayers adsorbed on Ni.

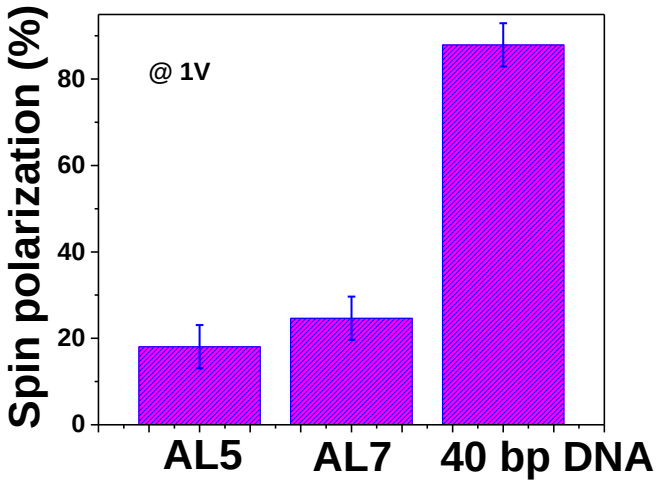

Figure S8. Spin polarization obtained at 1 V using difference in the current of the two spins over the sum.

Photoelectrochemistry

To investigate the effects of modifying the TiO_2 electrodes with different linker molecules on the photoelectrochemical process, we performed Mott-Schottky impedance spectroscopy measurements. Results from the Mott-Schottky impedance measurements are presented in Figure S9.

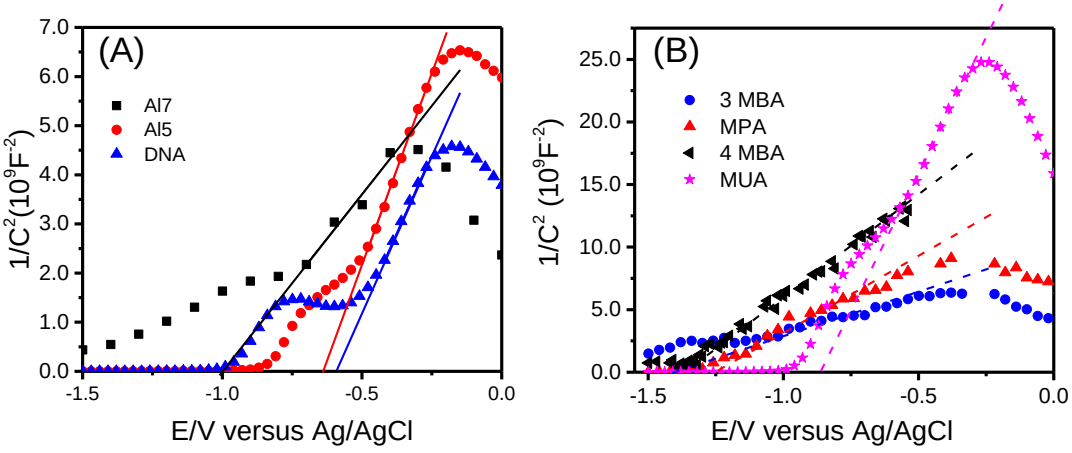

Figure S9: Mott-Schottky plots of TiO_2-modified electrodes to determine the flat band potential. These measurements were performed in 1.0 M KCl (pH 5.45) at a frequency of 1 kHz and with an oscillation voltage of 25 mV.

To determine the flat band potential of each modified electrode, the linear part of the data can be fit to the equation,

$$\frac{1}{C^2} = \frac{2}{\varepsilon\varepsilon_0 q N_D}\left(E - E_{FB} - \frac{kT}{q}\right),$$

where C is the capacitance, N_D is the net doping density of TiO_2, E is the applied potential, and E_{FB} is the flat band potential. The flat band potential was obtained as an intercept to the horizontal axis where $^1/_{C^2} = 0$. The values presented in the table are averages obtained from several electrodes.

Photoelectrochemical measurements were performed in a three-electrode electrochemical cell, with Pt wire used as a counter electrode and with an Ag/AgCl (saturated KCl) reference electrode. A mixture of 0.35 M Na_2SO_3 and 0.25 M Na_2S aqueous solution (pH = 9.5) was used as the electrolyte. The Na_2S sacrificial reagent plays the role of hole scavenger, and is oxidized to S_2^{2-} to prevent the photocorrosion of CdSe.

To ensure efficient hydrogen production at the cathode, Na_2SO_3 was added to reduce disulfides back to sulfides, $S_2^{2-} + SO_3^{2-} = S^{2-} + S_2O_3^{2-}$, which has been shown to significantly increase the amount of hydrogen produced. A commercial Xe lamp with an intensity of 80 $mWcm^{-2}$ was used to illuminate the photoelectrodes. Linear scan voltammograms are presented in Figure S10.

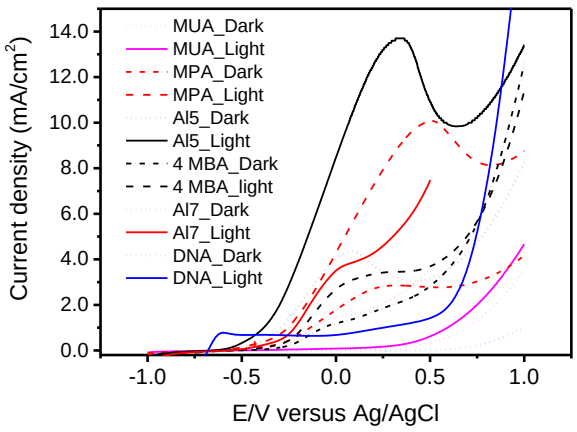

Figure S10: The current density as a function of the potential vs. the Ag/AgCl electrode

Hydrogen gas evolution was measured at various potentials using the Princeton potentiostat in the chronoamperometry mode, under light illumination. The produced hydrogen gas was measured in an air-tight H-cell. Potentials varying from 0.25 V to 0.70 V versus

Ag/AgCl were applied in the chronoamperometry mode to the working electrode while H_2 production was monitored on the cathode. Table S1 presents the observations noted.

Table S1: Applied potentials for effective collection of the produced hydrogen gas.

Electrode	Applied Potential vs Ag/AgCl (V)	H_2 production observed
TiO_2/Al5/CdSe	0.25	yes
	0.30	yes
	0.70	yes
TiO_2/Al7/CdSe	0.25	yes
	0.30	yes
	0.70	yes
TiO_2/DNA/CdSe	0.25	no
	0.30	yes
	0.70	yes
TiO_2/4MBA/CdSe	0.25	no
	0.30	yes
	0.70	yes
TiO_2/3MBA/CdSe	0.25	no
	0.30	yes
	0.70	yes
TiO_2/MUA/CdSe	0.25	no
	0.30	no
	0.70	yes
TiO_2/MPA/CdSe	0.25	no
	0.30	no
	0.70	yes

Based on the observations from Table S1, the minimum potential for each electrode was chosen and hydrogen production was monitored as a function of time. The data are presented in Figure 4 in the main article. The gas produced under photoelectrochemical conditions was qualitatively confirmed as hydrogen using gas chromatography (GC) equipped with a thermal

conductivity detector (TCD) and using a GowMac instrument with a 20′ × 1/8″ stainless steel column packed with a molecular sieve (5 Å) in series with a 4′ × 1/8″ stainless steel column packed with HayeSep T. The carrier gas was Ar, and the column temperature was maintained at *T*=120 °C. Prior to the measurements, the instrument was calibrated with a commercial high pure H_2 gas (Figure S10 black).

The peak at 1.57 min relates to all heavy gases present in the sample, whereas the peak at 4.91 min corresponds to hydrogen. The gas produced at 0.25 V vs. Ag/AgCl in an electrochemical cell was collected using a Hamilton syringe and injected into a GC column. As shown in Figure S11, it is clear that the gas produced at the Pt electrode in the photoelectrochemical cell is hydrogen.

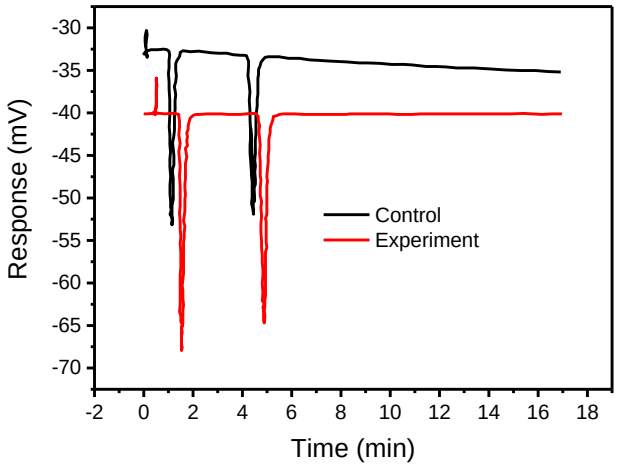

Figure S11: Gas chromatogram obtained from a pure hydrogen (commercial) sample injected into the gas chromatography chamber (black curve) and from a gas sample produced in the photoelectrochemical cell, injected into the gas chromatography chamber (red curve). The curves were displaced relative to each other to facilitate the comparison.

Hydrogen production with oligopeptides

Two oligopeptides were studied: L- (COOH)-(Ala-Aib)$_n$-NH-(CH$_2$)$_2$-SH when n=5 and 7. The yield of hydrogen production was by about a factor of 4.0 higher for the short oligomer (n=5). Figure S12 presents the hydrogen production with the long oligomer at 0.25 and 0.40 V versus Ag/AgCl. Although the yield here is lower than with the shorter oligopeptide, hydrogen is produced at over-potential as low as 0.25.

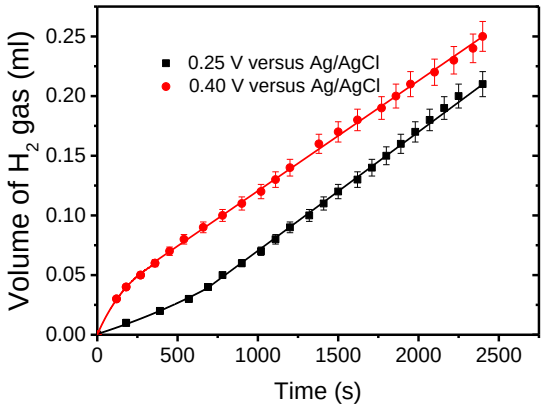

Figure S12: The hydrogen production as a function of time for two over-potentials, when the electrode used contained the long oligopeptide $SHCH_2CH_2CO$-(Ala-Aib)$_7$-COOH.

Open circuit potential (OCP)

The OCP values were measured for the cells containing the different molecules. Typically, the light effect on the OCP is small, with 4MBA being the exception (see Table S2). This is due to the efficient light induced electron transfer through this molecule. There is no significant difference between the OCP values obtained with chiral or achiral molecules, as expected.

Table S2: The open circuit potential (OCP) measured at dark and the photo-induced OCP.

Molecule	OCP [dark] (V)	OCP [light-dark] (V)
Al7	0.80	0.1
Al5	0.55	0.02
DNA	-0.12	0.03
MUA	1.1	-0.07
MPA	-0.14	0.04
4MBA	0.58	-0.46

References

(1) Salant, A.; Shalom, M.; Hod, I.; Faust, A.; Zaban, A.; Banin, U. *ACS Nano,* **2010,** *4*, 5962.

(2) Li, X.; Qiu, Y.; Wang, S.; Lu, S.; Gruar, R. I.; Zhang, X.; Darr, J. A.; He, T. *Phys. Chem. Chem. Phys*. **2013**, *15*, 14729.

(3) Yum, J-H.; Kim, S-S.; Kim D-Y.; Sung Y-E. *J. Photochem. and Photobiology A: Chemistry.* **2005**, *173*, 1.

(4) Fukada, Y.; Nagarajan, N.; Mekky, W.; Bao, Y.; Kim, H.-S.; Nicholson, P. S. *J. Mater. Sci.* **2004**, *39*, 787.

(5) Besra, L.; Liu, M. *Prog. Mat. Sci.* **2007**, *52*, 1.

(6) Mann, J. R.; Watson, D. *Langmuir* **2007**, *23*, 10924-10928.

(7) Chen, J.; Franking, R.; Ruther, R. E.; Tan, Y.; He, X.; Hogendoorn, R. S.; Hamers, R. J. *Langmuir*. **2011**, *27*, 6879.

(8) Titheridge, D. J.; Barteau, M. A.; Idriss, H. *Langmuir*. **2001**, *17*, 2120.

(9) Nogues, C.; Cohen, S. R.; Daube, S. S.; Naaman, R. *Phys.Chem.Chem.Phys.* **2004,** *6*, 4459.

(10) Xie, Z.; Markus, T. Z.; Cohen, S. R.; Vager, Z.; Gutierrez, R.; Naaman, R. *Nano Lett*. **2011**, *11*, 4652.

(11) Kettner, M.; Göhler, B.; Zacharias, H.; Mishra, D.; Kiran, V.; Naaman, R.; Fontanesi, C.; Waldeck, D. H.; Sęk, S.; Pawłowski, J.; Juhaniewicz, J. *J. Phys. Chem. C*. **2015**, *119*, 14542.

(12) Kitagawa, K.; Morita, T.; Kimura, S. *Angew Chem Int. Ed.* **2005**, *44*, 6330.